Preprints of the 21st IFAC World Congress (Virtual)
Berlin, Germany, July 12-17, 2020

Demand Tracking Control in Manufacturing Systems

Khaled A.A.A. Othman **Thomas Meurer**

Chair of Automatic Control, Faculty of Engineering, Kiel University, 24143 Kiel, Germany (e-mail: {kao,tm}@tf.uni-kiel.de).

Abstract: The purpose of this research is to design optimal boundary control to solve demand tracking problems for manufacturing systems represented at the factory level in terms of conservation laws coupled with ordinary differential equations. The factory level is modeled as a network with arcs describing specific production policies, e.g., velocity, processing rate, number of machines, and each vertex represents the buffer zone. Different interconnection topologies that correspond to dispersing and merging networks are considered. Numerical solutions are performed using direct and indirect methods.

Keywords: Manufacturing systems, Production systems, Flow control, Conservation laws, Boundary control, Optimal control, Continuum models.

1. INTRODUCTION

Production flow control is one of the key operations to solve issues such as cost reduction, energy savings, optimizing machines utilization, and time savings and leads to maximize profit in manufacturing systems.

In general three main modeling approaches are available for manufacturing systems: discrete event models, see, e.g., Lauzon et al. (1996), fluid models, see, e.g., Panayiotou and Cassandras (2006) and queuing models, see, e.g., Papadopoulos and Heavey (1996). Typically, discrete event models are stochastic models to describe the dynamics of manufacturing systems. However, the main drawback, as declared in Fishwick (2007), is that it is difficult to design a controller in case of a large or complex system that contains a large amount of information (states). Fluid models are flux oriented and are typically represented by ordinary differential equations (ODEs). The main shortcoming of fluid models is that these models do not express flow times which means that the flux can be produced using zero inventory (van den Berg et al., 2008). Besides, these models are not suitable for modeling the complete dynamic behavior (transient and steady state) of a manufacturing system. Queuing models show the connection between throughput and flow time only in steady state which is not applicable for control theory. Recently, partial differential equations (PDEs) have been utilized for modeling of manufacturing systems. The main idea comes from the continuum theory of highway traffic (Lighthill and Whitham, 1955), (Richards, 1956). The motivation for using PDE models is that these are suitable for a proper controller design by considering that the lots are produced continuously on large scale manufacturing systems. Also, PDE models are computationally feasible and express the complete behavior of the dynamic system by incorporating the system characteristics of both throughputs and flow times. Therefore, PDE models are adopted in the present paper.

Several hyperbolic PDEs models have been proposed by Armbruster et al. (2003) and Lefeber (2004). These models have been validated by comparison with discrete event systems in van den Berg et al. (2008) and model predictive control (MPC) is employed to solve both tracking and backlog problems for homogeneous (identical) machines in the manufacturing system. The adjoint state method as an optimal control for re-entrant homogeneous manufacturing system characterized by non-local velocity (spatial invariant) is used by La Marca et al. (2010). Armbruster et al. (2006) deduced that the mass conservation law is asymptotically valid in the supply chain network with a large number of lots. The purpose is to construct a simplified formula of the relation between the density and the flux on a large scale. This model has been modified by Göttlich et al. (2006) by coupling ODEs to PDEs, which represents the supply chain network to avoid the occurrence of bottlenecks. Optimal control is applied to this model using adjoint equations in comparison with a mixed-integer programming (MIP) to minimize the flow or maximize it in certain locations inside the network (Kirchner et al., 2006). Moreover, feedback control laws are applied based on Boltzmann equations to allow supply chain models to deal with priorities (Herty and Ringhofer, 2011). Besides, the investigation of the feedback stabilization for a production model is using a Lyapunov argument (Baumgärtner et al., 2019). Having these studies as point of departure, the main contribution of the present paper is to apply optimal control using the adjoint technique to optimize the tracking of desired demand trajectories based on quasi-linear hyperbolic PDEs coupled with ODEs models. These models represent the entire network at the factory level.

The paper is organized as follows: Sec. 2 introduces the problem setting. Sec. 3 presents two different optimization approaches to solve the problem. Sec. 4 shows the parameter setup and discusses the simulation results. Sec.

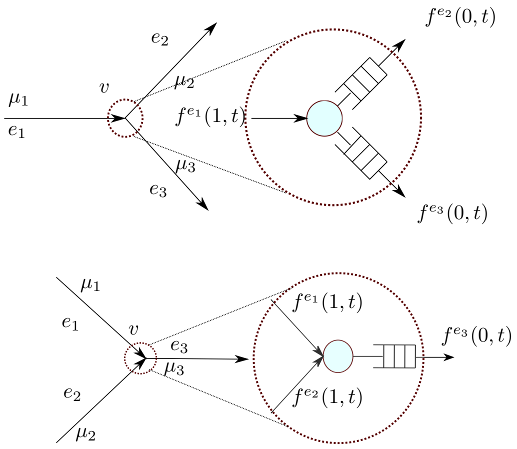

Fig. 1. Dispersing network (top) and merging network (bottom).

5 presents the example of the complex network. Sec. 6 provides the conclusion of the paper.

2. PROBLEM STATEMENT

The system consists of flow lines with each having an identical number of workstations. Each workstation includes a machine and a buffer. The production flow works according to an M/M/1 model, which means process time and inter-arrival time are exponentially distributed. The flow line is represented by the arc e and modeled as a single PDE. Between two successive arcs there is a storage area represented by vertex v and modeled as a single ODE. The importance of the vertex is to keep the incoming flow lower than the processing rate in each arc. In the network context, these components are connected to construct a dispersing network or a merging network as shown in Fig. 1. The position of the workstation inside each arc is denoted by the normalized coordinate $x \in [0, 1]$. The inlet of the arc e is at $x = 0$ and at $x = 1$ is the outlet of the same arc. The buffer zone is located between the exit of a specific arc and the entrance of a succeeding arc. The following assumptions are imposed: (i) the lots are conserved inside the arcs, (ii) the density of lots $\rho^e(x,t)$ and the flux $f^e(x,t)$ are non-negative, (iii) each queue is considered to follow a first-in-first-out (FIFO) policy and has infinite capacity. The task of the storage area at vertex v is to compensate for the difference between the incoming flows from the outlets of the predecessor arcs and the outgoing flows to the successor arcs by storing the lots. The system dynamics for each flow line e can be described as

$$
\begin{aligned}
\frac{\partial}{\partial t}\rho^e(x,t) &= -\frac{\partial}{\partial x} f^e(\rho^e(x,t)),\\
f^e(\rho^e(x,t)) &= \rho^e v^e = \frac{\mu^e \rho^e(x,t)}{M^e + \rho^e(x,t)}.
\end{aligned}
\tag{1}
$$

Each arc e is an aggregated PDE model with individual properties such as the mean processing rate μ^e for each machine and the number of the machines or workstations M^e. The structure of the buffer zone at v differs depending on the network topology. For the dispersing network shown in Fig. 1 (top) the PDE model (1) is amended by

$$
\begin{gathered}
\frac{dq_v^{e^+}(t)}{dt} = A_v^{e^+}(t) f^{e^-}(1,t) - f^{e^+}(0,t),\\
f^{e^+}(0,t) = \min\left(\mu^{e^+}, \frac{q_v^{e^+}(t)}{\kappa}\right),\\
\rho^e(x,0) = 0, \quad q_v^e(0) = 0, \quad f^{e_1}(0,t) = u(t)\\
0 \le A_v^{e^+}(t) \le 1,\ \sum A_v^{e^+}(t) = 1,\ 0 \le u(t) < \mu^{e_1}\\
e^- \in \{1\}, \quad e^+ \in \{2,3\}, \quad v \in \{1\}.
\end{gathered}
\tag{2}
$$

Herein, $\frac{dq_v^{e^+}(t)}{dt}$ is the rate of the change of the buffer load. The arcs e^- and e^+ refer to the arcs before and after the vertex, respectively. The parameter κ is a smoothing parameter. The outflow from arc e_1 splits into two flows. The summation of these flows must be equal to the outflow coming from e_1 which is covered by the fraction $A_v(t) \in [0, 1]$ and the conditions in (2). At the initial time $t = 0$, it is assumed that no lots are inside the system. Besides, the incoming flow is bounded between zero and the processing rate of each arc.

For a merging network according to Fig. 1 (bottom) the PDE model (1) is subject to

$$
\begin{gathered}
\frac{dq_v^{e^+}(t)}{dt} = A_v(t) \sum_{e^- \in \{1,2\}} f^{e^-}(1,t) - f^{e^+}(0,t),\\
f^{e^+}(0,t) = \min\left(\mu^{e^+}, \frac{q_v^{e^+}(t)}{\kappa}\right),\\
\rho^e(x,0) = 0, \quad q_v^{e^+}(0) = 0, \quad f^{e_1}(0,t) = u(t)\\
0 \le u(t) < \mu^{e_1}, \quad 0 \le A_v(t) \le 1\\
e^- \in \{1,2\}, \quad e^+ \in \{3\}, \quad v \in \{1\}.
\end{gathered}
\tag{3}
$$

Here, all incoming flows are combined together to enter the main arc e_3. The value $A_v(t) \in [0, 1]$ denotes a fraction of the entire incoming flows at vertex v. This part is crucial because it means that some unrequired lots are stored in the storage area.

3. OPTIMAL CONTROL APPROACHES

To control the flow on the network along a prescribed desired outflow trajectory subsequently optimal control is applied by considering the objective functional

$$
\min_{u, A_v} J(u, A_v) = \frac{1}{2}\int_0^{t_f} (y(t) - f^*(t))^2 dt, \tag{4}
$$

subject to (1), (2) for the dispersing or (1), (3) for the merging network, respectively. Here, $f^*(t)$ is the desired trajectory and $y(t) = f^{e_3}(1,t)$ is the outflow from the arc e_3 to fix the control problem in the dispersing and the merging scenarios. To solve the optimal control problem direct and indirect methods are utilized and compared.

3.1 Direct Method

In the direct approach both the PDE (1) describing the state evolution along each arc and the ODEs arising in (2) or (3), respectively, are fully discretized. For this, an upwind scheme is used for spatial discretization, and the explicit Euler method is applied for time discretization. Let $\Delta x = 1/M^e$ and Δt denote the spatial and time step where Δt and Δx are connected by the Courant-Friedrichs-Lewy condition $CFL = \frac{V_m^e dt}{dx} \leq 1$ for numerical stability purposes with V_m^e the maximum speed in each arc. In addition introduce $\rho_{i,j}^e = \rho^e(i\Delta x, j\Delta t)$, $f_{i,j}^e = f^e(i\Delta x, j\Delta t)$, $q_{v,j}^{e^+} = q_v^{e^+}(j\Delta t)$, $y_j = y(j\Delta t)$, $u_j = u(j\Delta t)$, $A_{v,j} = A_v(j\Delta t)$ for $i = 1, 2, \ldots, M^e$, $j = 0, 1, \ldots, N-1$. Taking into account the discretization of the objective functional (4) the static optimization problem is obtained consisting of

$$\min_{u, A_v} J(u, A_v) = \frac{1}{2} \sum_{j=0}^{N} (y_j - f_j^*)^2 \Delta t, \tag{5}$$

subject to

$$\begin{aligned}
\rho_{i,j+1}^e &= \rho_{i,j}^e - \frac{\Delta t}{\Delta x}(f_{i,j}^e - f_{i-1,j}^e), \\
q_{v,j+1}^{e_2} &= q_{v,j}^{e_2} + \Delta t\Big(A_{v,j} f_{M^e,j}^{e_1} - f_{0,j}^{e_2}\Big), \\
q_{v,j+1}^{e_3} &= q_{v,j}^{e_3} + \Delta t\Big((1 - A_{v,j}) f_{M^e,j}^{e_1} - f_{0,j}^{e_3}\Big), \\
f_{0,j}^{e^+} &= \min\left(\mu^{e^+}, \frac{q_{v,j}^{e^+}}{\kappa}\right), \\
\rho_{i,0}^e &= 0, \quad q_{v,0}^{e^+} = 0, \quad f_{0,j}^{e_1} = u_j \\
e^+ &\in \{2, 3\}, \quad 0 \leq u_j < \mu^{e_1}, \quad 0 \leq A_{v,j} \leq 1,
\end{aligned} \tag{6}$$

for the dispersing network. In case of the merging network (5) is extended by

$$\begin{aligned}
\rho_{i,j+1}^e &= \rho_{i,j}^e - \frac{\Delta t}{\Delta x}(f_{i,j}^e - f_{i-1,j}^e), \\
q_{v,j+1}^{e^+} &= q_{v,j}^{e^+} + \Delta t\Big(A_{v,j} \sum_{e^- \in \{1,2\}} f_{M^e,j}^{e^-} - f_{0,j}^{e^+}\Big), \\
f_{0,j}^{e^+} &= \min\left(\mu^{e^+}, \frac{q_{v,j}^{e^+}}{\kappa}\right), \\
\rho_{i,0}^e &= 0, \quad q_{v,0}^{e^+} = 0, \quad f_{0,j}^{e_1} = u_j \\
e^+ &\in \{3\}, \quad 0 \leq u_j < \mu^{e_1}, \quad 0 \leq A_{v,j} \leq 1.
\end{aligned} \tag{7}$$

The optimization problem is solved using SQP method by making use of MATLAB. The control variables u_j and $A_{v,j}$ are needed as an initial guess to solve the problem. In each iteration, the gradient is updated by finding a new step length and search direction.

3.2 Indirect Method

In this approach, the optimization is performed for the infinite-dimensional system. The Lagrangian L of problem (4) for the dispersing network is obtained as

$$\begin{aligned}
L = {} & \frac{1}{2} \int_0^{t_f} (y(t) - f^*(t))^2 dt \\
+ & \sum_{e \in \{1,2,3\}} \int_0^{t_f} \int_0^1 \lambda^e \Big(\frac{\partial}{\partial t}\rho^e + \frac{\partial}{\partial x} f^e(\rho^e)\Big) dx dt \\
+ & \sum_{e^+ \in \{2,3\}} \int_0^{t_f} \phi_v^{e^+} \Big(\dot{q}_v^{e^+} - A_v^{e_3} f^{e^-}(1,t) + f^{e^+}(0,t)\Big) dt.
\end{aligned} \tag{8}$$

For the merging network L is obtained as

$$\begin{aligned}
L = {} & \frac{1}{2} \int_0^{t_f} (y(t) - f^*(t))^2 dt \\
+ & \sum_{e \in \{1,2,3\}} \int_0^{t_f} \int_0^1 \lambda^e \Big(\frac{\partial}{\partial t}\rho^e + \frac{\partial}{\partial x} f^e(\rho^e)\Big) dx dt \\
+ & \int_0^{t_f} \phi_v^{e^+} \Big(\dot{q}_v^{e^+} - A_v \sum_{e^- \in \{1,2\}} f^{e^-}(1,t) + f^{e^+}(0,t)\Big) dt.
\end{aligned} \tag{9}$$

The functions $\lambda^e(x,t)$ and $\phi_v^{e^+}(t)$ are the adjoint states for the equality constraints induced by the PDEs on the arcs and the ODEs at the vertices, respectively. Evaluating the Gateaux derivative of L, applying integration by parts and regrouping one obtains

$$\begin{aligned}
\frac{\partial}{\partial t}\lambda^e &= -\left(\frac{\mu^e M^e}{(M^e + \rho^e(x,t))^2}\right) \frac{\partial}{\partial x}\lambda^e, \\
\lambda^e(x, t_f) &= 0, \\
\lambda^{e_3}(1,t) &= f^*(t) - y(t), \\
\phi_v^{e^+}(t) &= \lambda^{e_3}(0,t).
\end{aligned} \tag{10}$$

The difference between the dispersing and the merging networks is found in the coupling and the variational derivatives with respect to the control variables. Hence, in case of the dispersing scenario this implies

$$\begin{aligned}
\lambda^{e_1}(1,t) &= \lambda^{e_3}(0,t) A_v^{e_3}(t), \\
\delta_u J(t) &= -\lambda^{e_1}(0,t), \\
\delta_{A_v^{e_3}} J(t) &= -\lambda^{e_3}(0,t) f^{e_1}(1,t).
\end{aligned} \tag{11}$$

For the merging scenario one obtains

$$\begin{aligned}
\lambda^{e_1}(1,t) &= A_v(t) \lambda^{e_3}(0,t), \\
\delta_u J(t) &= -\lambda^{e_1}(0,t), \\
\delta_{A_v} J(t) &= -\lambda^{e_3}(0,t)(f^{e_1}(1,t) + f^{e_2}(1,t)).
\end{aligned} \tag{12}$$

The system dynamics (1), (2) or (1), (3), respectively are discretized and solved forward in time as in (6) or (7), respectively. The adjoint equations are discretized and solved backward in time for $i = M^e - 1, \ldots, 1, 0$, $j = N, \ldots, 2, 1$ according to

$$\begin{aligned}
\lambda_{i,j-1}^e &= \lambda_{i,j}^e - \frac{\Delta t}{\Delta x}\left(\frac{\mu^e M^e}{(M^e + \rho_{i,j}^e)^2}\right)(\lambda_{i+1,j}^e - \lambda_{i,j}^e), \\
\lambda_{i,N}^e &= 0, \\
\lambda_{M^e,j}^{e_3} &= f_j^* - y_j, \\
\phi_{v,j}^{e^+} &= \lambda_{0,j}^{e_3}.
\end{aligned} \tag{13}$$

The discretized form of (11) in the dispersing network becomes

$$\begin{aligned}
\lambda_{M^e,j}^{e_1} &= \lambda_{0,j}^{e_3} A_{v,j}^{e_3}, \\
\delta_u J_j &= -\lambda_{0,j}^{e_1}, \\
\delta_{A_v^{e_3}} J_j &= -\lambda_{0,j}^{e_3} f_{M^e,j}^{e_1}.
\end{aligned} \tag{14}$$

While for the merging network (12) implies

$$\begin{aligned}
\lambda_{M^e,j}^{e_1} &= A_{v,j} \lambda_{0,j}^{e_3}, \\
\delta_u J_j &= -\lambda_{0,j}^{e_1}, \\
\delta_{A_v} J_j &= -\lambda_{0,j}^{e_3}(f_{M^e,j}^{e_1} + f_{M^e,j}^{e_2}).
\end{aligned} \tag{15}$$

The gradients are then computed from (14) or (15), respectively, and are combined with an SQP approach to find local minimizers $u^*(t)$ and $A_v^*(t)$.

4. SIMULATION RESULTS

In this section, controlled and uncontrolled networks are studied. For the dispersing network with three arcs the the number of machines in each arc is chosen as $M^e = 10$ with the processing rates μ^e being 2, 3 and 4 in e_1, e_2 and e_3 respectively. In case of the merging network $\mu^{e_1} = 4$, $\mu^{e_2} = 3$ and $\mu^{e_3} = 2$ are used. The spatial step size $\Delta x = 0.1$ in each are e and CFL is 0.5. For the uncontrolled networks $A_v^{e_2}(t) = 0.7$, $A_v^{e_3}(t) = 0.3$ and the smoothing factor is chosen as $\kappa = 0.2$. The aim is to show the dynamics of the uncontrolled network.

4.1 Dispersing Network

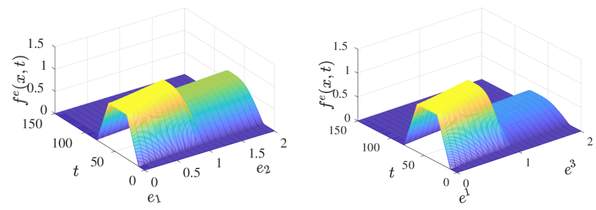

Fig. 2. Flux evolution through arcs e_1, e_2 (left) and e_1, e_3 (right) for uncontrolled dispersing network.

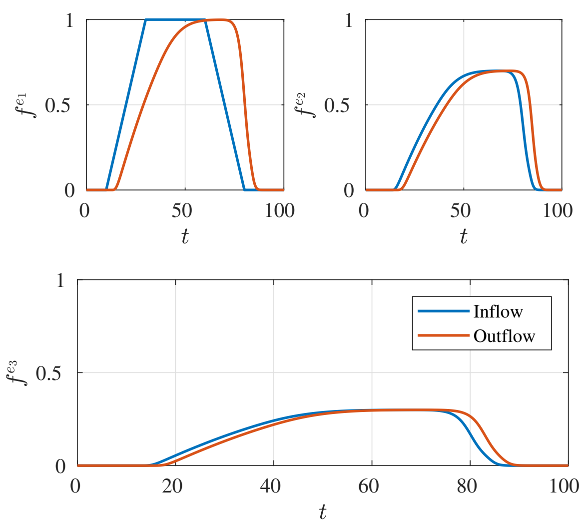

Fig. 3. Flux in each arc at the inlet and the outlet in the uncontrolled dispersing network.

In case of the uncontrolled dispersing network, Fig. 2 shows the evolution of the flux inside the network. The inflow profile is applied at $x = 0$ and the flux grows in arc e_1 as is shown in Fig 3 (top-left). From the numerical results, the lots are conserved along the system. This is checked by integrating both the inflow and the outflow of each arc with respect to time in the time interval. The total number of lots at the inlet of the arc e_1 equals 50. These are split into 35 and 15 lots passing arcs e_2 and e_3, respectively.

In the controlled dispersing network, both direct and indirect approaches are utilized. In case of the dispersing network the final value of the objective functional (4) is

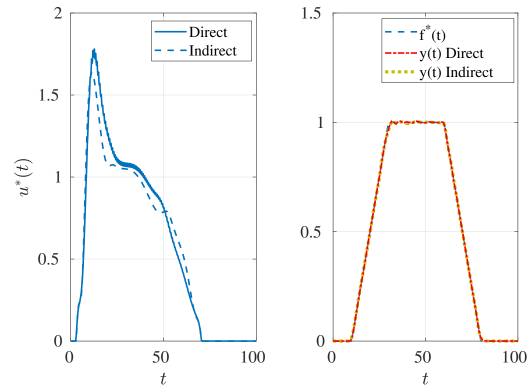

Fig. 4. Input $u^*(t)$ (left) and comparison of the desired demand trajectory $f^*(t)$ and $f^{e_3}(1,t)$ (right) in case of direct and indirect method.

1.03×10^{-3} by the direct method reasonably well demand tracking is achieved. As is shown in Fig. 4 the input from the indirect method is smoother than the input from the direct method and the output in arc e_3 perfectly matches the desired flow trajectory. The final value of the objective functional (4) is 7.29×10^{-4}.

4.2 Merging Network

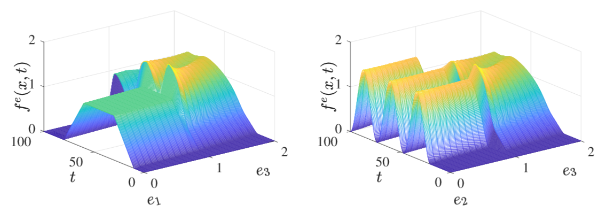

Fig. 5. Flux evolution through arcs e_1, e_2 (left) and e_1, e_3 (right) in the uncontrolled merging network.

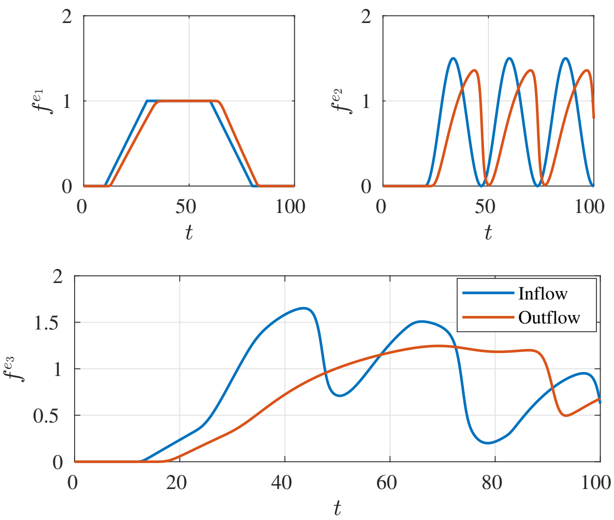

Fig. 6. Flux in each flow line e_1, e_2 and e_3 in the uncontrolled merging network.

For the case of the uncontrolled merging network, the imposed boundary inflows in e_1 and e_2 are shown in Fig.

5. In arc e_2 the outflow can not reach the maximum of the inflow level because of the processing rate μ^{e_2}. The processing rate plays an important role in the system utilization $utl^e = \frac{u^e}{\mu^e}$. The higher the processing rate, the lower the utilization. The lots are still under processing in the arc. Here, the difference between the inflow and the outflow is not equal to zero. The same also occurs in arc e_3. For example, the total number of lots entering e_3 is 71 with 67 leaving the arc at the outlet and the lots being processed is 4. The conservation of mass holds anywhere in the system except inside the storage area.

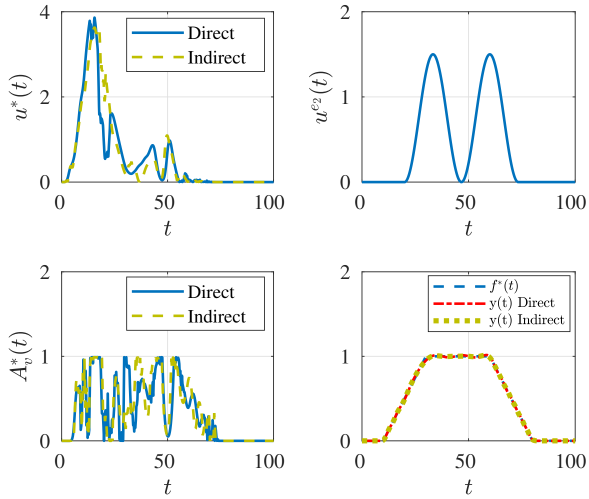

Fig. 7. Direct and indirect approaches used for demand tracking in the merging network.

By applying the direct approach in the merging network, the outflux is reasonably tracking the desired demand, see Fig. 7. However, it slightly oscillates in steady state region from the time ranging between 30 to 60 unit of time. The final value of the objective functional equals 4.19×10^{-3} for the direct method and 3.19×10^{-3} for the indirect method. The outflux matches the desired demand, especially in both ramp-up and ramp-down behaviours.

5. EXAMPLE OF COMPLEX NETWORK

The control problem (4) is considered for a complex network as shown in Fig. 8. Herein, the inflow to the system at the inlet of arc e_1 is $u(t) = f^{e_1}(0, t)$ and the outflow $y(t) = f^{e_7}(1, t)$ is the outlet of the arc e_7. The parameters of the network are chosen as $\kappa = 0.25$, $M^e = 10$, $\mu^{e_1} = 6$, $\mu^{e_2} = 4$, $\mu^{e_3} = 3$, $\mu^{e_4} = 2$, $\mu^{e_5} = 3$, $\mu^{e_6} = 4$, and $\mu^{e_7} = 5$. The control variables are the inflow and the fractions of the vertices $u(t)$, $A_{v1}(t)$, $A_{v2}(\mathrm{t})$, $A_{v3}(t)$ and $A_{v4}(t)$ respectively.

The results in Fig. 9 for the indirect method show that the outflow completely with the desired trajectory in all states. The final value of the objective functional is 1.01×10^{-3}. With the direct method, the mismatch between the outflow and the desired flow becomes obvious, especially in ramp-up and ramp-down regions compared to the indirect method, see Fig. 10. The final value of the objective

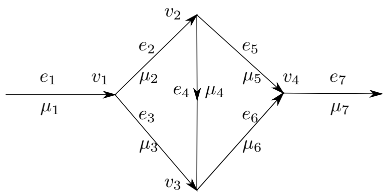

Fig. 8. The structure of the complex network.

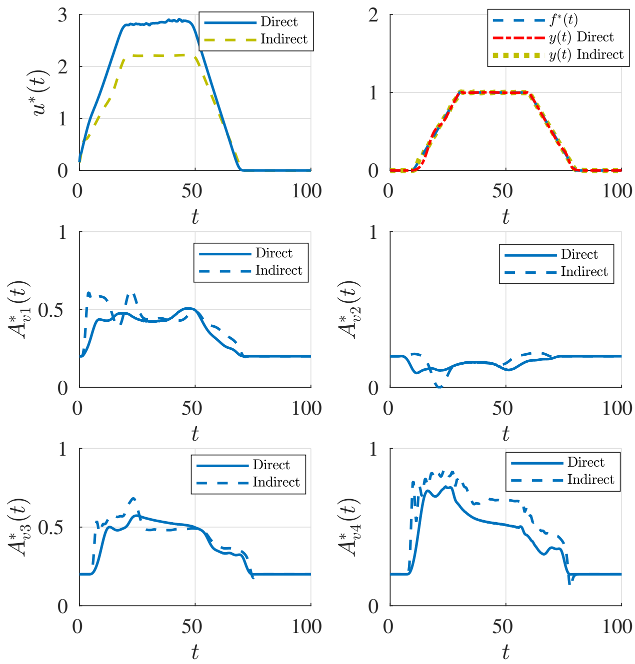

Fig. 9. Direct and indirect approaches used for demand tracking in the complex network.

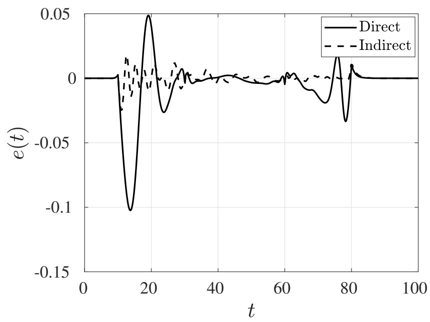

Fig. 10. The error $e(t)$ between $y(t)$ and $f^*(t)$ in case of complex network using direct and indirect methods.

functional equals 2.36×10^{-2} in case of the direct method.

In general, the results in the indirect method are more satisfactory than the ones obtained for the direct method and the outflow perfectly matches the desired demand trajectory in the operational time interval. According to the fixed parameter setup in both methods, the simulation time using the indirect method is shorter than using the direct one in all situations merging, dispersing and complex networks.

6. CONCLUSION

Demand tracking control in manufacturing systems is studied using an optimal control approach. The flow lines (arcs) are modeled as PDEs. The storage areas (vertices) are modeled by ODEs. These PDEs and ODEs are coupled in different network topologies at the factory level, which is constructed for two simple dispersing and merging networks and a more complex network. In each case, a direct method and an indirect method are applied to solve the optimal control problem addressing demand tracking. For this a desired reference trajectory is assigned to the outlet of a particular arc depending on the network topology. Although both approaches provide satisfactory results the obtained numerical results indicate that the indirect method is more efficient and accurate.

ACKNOWLEDGEMENTS

The authors acknowledge the Egyptian Ministry of Education (Cultural Affairs and Missions Sector) for financial support during this work.

REFERENCES

Armbruster, D., Degond, P., and Ringhofer, C. (2006). A model for the dynamics of large queuing networks and supply chains. *SIAM Journal on Applied Mathematics*, 66(3), 896–920.

Armbruster, D., Marthaler, D., and Ringhofer, C. (2003). Kinetic and fluid model hierarchies for supply chains. *Multiscale Modeling & Simulation*, 2(1), 43–61.

Baumgärtner, V., Göttlich, S., and Knapp, S. (2019). Feedback stabilization for a coupled pde-ode production system. *arXiv preprint arXiv:1903.11507*.

Fishwick, P.A. (2007). *Handbook of dynamic system modeling*. CRC Press.

Göttlich, S., Herty, M., Klar, A., et al. (2006). Modelling and optimization of supply chains on complex networks. *Communications in Mathematical Sciences*, 4(2), 315–330.

Herty, M. and Ringhofer, C. (2011). Feedback controls for continuous priority models in supply chain management. *Computational Methods in Applied Mathematics Comput. Methods Appl. Math.*, 11(2), 206–213.

Kirchner, C., Herty, M., Göttlich, S., and Klar, A. (2006). Optimal control for continuous supply network models. *NHM*, 1(4), 675–688.

La Marca, M., Armbruster, D., Herty, M., and Ringhofer, C. (2010). Control of continuum models of production systems. *IEEE Transactions on Automatic Control*, 55(11), 2511–2526.

Lauzon, S., Ma, A., Mills, J., and Benhabib, B. (1996). Application of discrete-event-system theory to flexible manufacturing. *IEEE Control Systems Magazine*, 16(1), 41–48.

Lefeber, E. (2004). Nonlinear models for control of manufacturing systems. *Nonlinear Dynamics of Production Systems*, 69–81.

Lighthill, M.J. and Whitham, G.B. (1955). On kinematic waves. ii. a theory of traffic flow on long crowded roads. In *Proceedings of the Royal Society of London A: Mathematical, Physical and Engineering Sciences*, volume 229, 317–345. The Royal Society.

Panayiotou, C. and Cassandras, C.G. (2006). Infinitesimal perturbation analysis and optimization for make-to-stock manufacturing systems based on stochastic fluid models. *Discrete Event Dynamic Systems*, 16(1), 109–142.

Papadopoulos, H. and Heavey, C. (1996). Queueing theory in manufacturing systems analysis and design: A classification of models for production and transfer lines. *European Journal of Operational Research*, 92(1), 1–27.

Richards, P.I. (1956). Shock waves on the highway. *Operations Research*, 4(1), 42–51.

van den Berg, R., Lefeber, E., and Rooda, K. (2008). Modeling and control of a manufacturing flow line using partial differential equations. *IEEE Transactions on Control Systems Technology*, 16(1), 130–136.